

# STAR: SCALE-WISE TEXT-TO-IMAGE GENERATION VIA AUTO-REGRESSIVE REPRESENTATIONS

Xiaoxiao Ma<sup>1,3\*</sup>, Mohan Zhou<sup>2,3\*</sup>, Tao Liang<sup>3</sup>, Yalong Bai<sup>3</sup>, Tiejun Zhao<sup>2</sup>, Huaian Chen<sup>1†</sup>, Yi Jin<sup>1†</sup>,

<sup>1</sup>University of Science and Technology of China <sup>2</sup>Harbin Institute of Technology <sup>3</sup>Du Xiaoman  
 {xiao\_xiao, anchen}@mail.ustc.edu.cn, {mhzhou99, ylbai}@outlook.com,  
 {liangtao}@duxiaoman.com, jinyi08@ustc.edu.cn



Figure 1: Generated samples from text prompts. We show 512×512 samples.

## ABSTRACT

We present STAR, a text-to-image model that employs scale-wise auto-regressive paradigm. Unlike VAR, which is limited to class-conditioned synthesis within a fixed set of predetermined categories, our STAR enables text-driven open-set generation through three key designs: To boost diversity and generalizability with unseen combinations of objects and concepts, we introduce a pre-trained text encoder to extract representations for textual constraints, which we then use as guidance. To improve the interactions between generated images and fine-grained textual guidance, making results more controllable, additional cross-attention layers are incorporated at each scale. Given the natural structure correlation across different scales, we leverage 2D Rotary Positional Encoding (RoPE) and tweak it into a normalized version. This ensures consistent interpretation of relative positions across token maps at different scales and stabilizes the training process. Extensive experiments demonstrate that STAR surpasses existing benchmarks in terms of fidelity, image text consistency, and aesthetic quality. Our findings emphasize the potential of auto-regressive methods in the field of high-quality image synthesis, offering promising new directions for the T2I field currently dominated by diffusion methods. Available at <https://github.com/krennic999/STAR>.

## 1 INTRODUCTION

Text-to-Image (T2I) generation has emerged as a major trend in recent computer vision community. With advancements in understanding textual instructions and producing realistic and imaginative

\*Equal contribution; † Corresponding author.

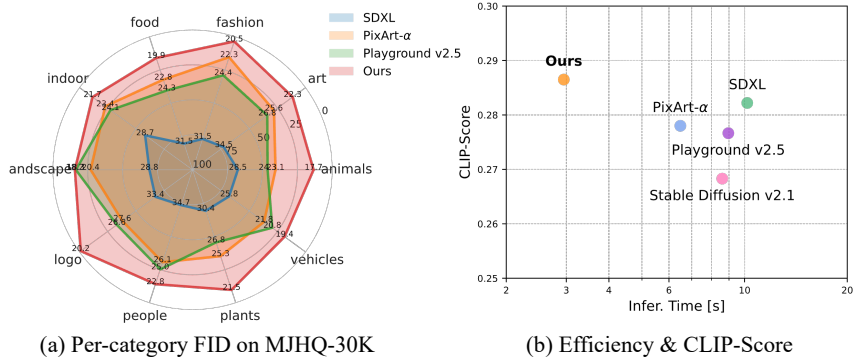


Figure 2: Comparison with current T2I methods. (a) Our STAR shows great fidelity on all categories in MJHQ-30K (b) and perform well in text-image alignment with reduced inference time on  $512 \times 512$  image generation.

images. This technology allows individuals to actualize their creative visions through digital painting and even has the power to change labor-intensive works, including secondary creations, virtual try-ons, and prototype design. This revolutionary capability is mainly supported by two mainstream generative paradigms in the current T2I pipeline:

**(1) Latent Variable Modeling.** Variational Auto-Encoder (Van Den Oord et al., 2017) (VAE), Generative Adversarial Network (GAN) (Karras et al., 2019; 2020) and Diffusion Model (OpenAI, 2023; Saharia et al., 2022; Rombach et al., 2022) (DM) operating by introduce an additional latent representation  $z$  with image  $x$ , then generate images through transformations from constrained prior  $p(z)$  or posterior  $p(z|x)$  under text guidance  $y$ . Specifically, VAEs explicitly constrain the posterior  $q(x|z)$  to fit in a normal distribution, which results in low-quality outcomes. GANs introduce a discriminator to measure the distance between generated and real images. While the min-max optimization of the generator and discriminator often fails due to mode collapse, leading to limited diversity. DMs adopt a more sophisticated way by gradually recovering image structure from noise, offering greater stability during training and more controllable outputs through cross-attention in each denoising step. Although diffusion models have demonstrated significant progress in various benchmarks and are widely used in current T2I applications, the “progressively” reconstruction process is time-consuming due to the lengthy sampling process.

**(2) Observed Variable Modeling.** In contrast to those latent-based methods, Auto-Regressive (AR) models (Yu et al., 2022a) aim to directly model the image distribution  $p(x)$  by generating tokens following a carefully-designed auto-regressive path, representing a fundamentally different paradigm. Traditional AR architectures such as PixelRNN, PixelCNN and GPT-like models propose to regress in image patches. They employ discrete image tokenizers such as VQ-VAE (Van Den Oord et al., 2017) and d-VAE (Ramesh et al., 2021) to convert 2D images into 1D patches, then utilize the next-token prediction optimization scheme akin to Large Language Models. However, these efforts often overlook the conflicts between the bi-directional and 2D structural correlations in image patch tokens and the unidirectional nature of AR models, leading to a degradation in quality. In contrast, VAR (Ramesh et al., 2021; Tian et al., 2024) reveals that the auto-regressive path is not only limited to patches. By introducing a multi-level VQ-VAE, images can be generated from token maps at different resolutions in a scale-wise manner, which is more suitable for auto-regressive modeling. VAR exhibits superiority in scale-wise generation over current state-of-the-art methods in ImageNet and patch-wise AR ones regarding scalability and computational efficiency.

However, it is important to note that the VAR framework is constrained to class-conditioned synthesis within a closed set of predetermined categories, and its effectiveness under textual conditions remains uncertain. To facilitate text-driven open-set generation, two crucial questions raise: 1) *How can textual guidance be effectively implemented?* VAR integrated category embedding to the initial start token, with guidance enhanced through adaptive layer-norm (AdaLN) layers. This approach causes insufficient fine-grained comprehension of textual information, resulting in poor controllability and failure when encountering unknown categories. 2) *How to handle various scales with a shared transformer?* Unlike traditional AR schemes that produce a single token per step, VAR must

produce a varying number of image tokens at each scale within an auto-regressive step. It ignores the correlation between image structures at different scales and employs learnable absolute positional encodings (APEs) at each scale. Consequently, this not only leads to parameter redundancy but also constrains its capabilities and application scope, results in sub-optimal optimization.

To alleviate this issue, we revisited the “next-scale prediction” mechanism in VAR, evolving it into general open-set T2I models for enhanced performance and efficiency, namely STAR. First, to boost diversity and generalizability with unseen combinations of objects and concepts, we introduce a pre-trained text encoder to extract representations for textual constraints, which we then use as guidance. Next, to improve the interactions between the generated images and fine-grained text guidance, making results more controllable, the additional cross-attention layers are incorporated at each scale. Finally, given the natural structure correlation across different scales, we leverage the 2D Rotary Positional Encoding (RoPE) (Su et al., 2024) and tweak it into a normalized version. This ensures consistent interpretation of relative positions across images at different scales and stabilizes the training process without APE parameters. Overall, as shown in Fig. 1, our STAR can generate images with enriched visual details, e.g., Animal hair, plant leaves, facial features, while demonstrating remarkable capability for fine-grained alignment with textual guidance (see Fig. 2).

The main contributions are summarized as follows:

1. We propose a novel auto-regressive model, STAR, for open-set text-to-image generation, which empowers the scale-wise paradigm introduced by VAR with the capability for text-conditioned image generation.
2. We employ features from pre-trained text encoder with cross attention layers for detailed textual guidance. Moreover, we develop a new normalized RoPE to enhance training effectiveness and ensure consistent interpretation of relative positions across different scales.
3. Extensive experiments and qualitative analysis are conducted to demonstrate the superiority of STAR over current methods. STAR achieves remarkable performance in fidelity, text-image consistency, particularly in producing highly detailed images with more efficiency.

## 2 RELATED WORKS

### 2.1 TEXT-TO-IMAGE (T2I) GENERATIVE MODELS

Current T2I models can be categorized into several types, *i.e.*, GAN, VAE, diffusion and Auto-regressive (AR) models. GANs (Xu et al., 2018; Tao et al., 2020; Kang et al., 2023) excel in producing vivid outcomes through adversarial training but often suffer from training instability. VAEs (Van Den Oord et al., 2017; Esser et al., 2021), on the other hand, explicitly constrain the posterior and decode samples from a normal distribution, resulting in lower generation quality.

Diffusion models (OpenAI, 2023; Saharia et al., 2022; Rombach et al., 2022) have notably surpassed GANs and VAEs in producing high-quality and diverse examples by learning a progressive denoising process (Dhariwal & Nichol, 2021). Further explorations in diffusion include new architecture designs (Song et al., 2020), acceleration (Luo et al., 2023), improved sampling quality (Ho & Salimans, 2022), and controllable generation (Zhang et al., 2023). Meanwhile, Diffusion Transformer (DiT) (Peebles & Xie, 2023) replaces U-Net in diffusion with transformer for enhanced quality. Implementations of DiT, such as PixArt (Chen et al., 2023a; 2024), SD3.0 (Esser et al., 2024) and SORA (Brooks et al., 2024), have demonstrated advancements in T2I synthesis. Although DiT offers scalability to some extent through transformer architecture, it struggles to achieve further performance gains (Tian et al., 2024), and multi-step denoising can be time-consuming.

### 2.2 AUTO-REGRESSIVE (AR) MODELS

The advancement of Large Language Models (LLMs) such as BERT (Lee & Toutanova, 2018), GPT (Radford et al., 2019; Brown et al., 2020) and LLama (Touvron et al., 2023a;b) has shown remarkable scalability (Zhang et al., 2022; Yu et al., 2022b) and zero-shot generalization (Sanh et al., 2021). These achievements inspires application of decoder-only transformer in visual generation tasks. Image tokenizers like VQGAN (Esser et al., 2021) or VQVAE (Van Den Oord et al., 2017) convert images into discrete tokens, which are sequentially predicted to create new images.

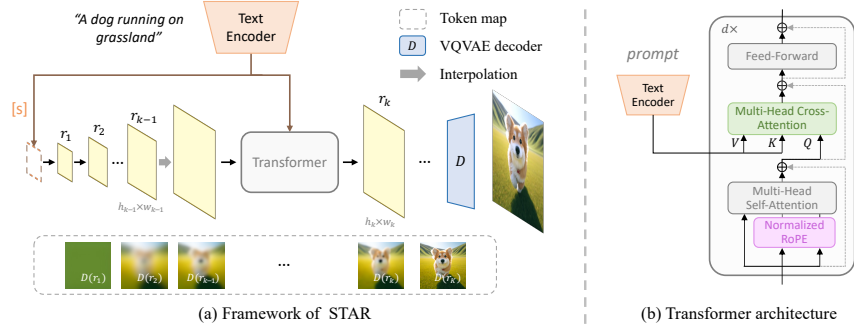


Figure 3: Illustration of proposed STAR. (a) From a text prompt, STAR generates images with pooled embeddings from a pre-trained text encoder and trains a transformer to gradually predicts token maps at a scale-wise manner. See in dashed box below, more details are gradually generated with detailed condition of text in each scale. (b) Normalized RoPE provides relative positions, and cross-attention is introduced for more detailed textual guidance.

Auto-regressive methods (Ramesh et al., 2021; Yu et al., 2022a; Gafni et al., 2022) in the style of GPT predict flattened token maps with raster scan, spiral order, *etc.*, in sequence. Make-A-Scene (Gafni et al., 2022) explores scene-based generation, while Parti (Yu et al., 2022a) scales up models and adopts ViT-VQGAN (Yu et al., 2021) for improved performance.

Despite their successes, the flatten of tokens poses a risk of potential structural degradation. In response, VAR (Tian et al., 2024) redefines the “order” by shifting from predicting tokens to token maps across different scales, providing better modeling of image and significantly enhanced scalability. This allows auto-regressive models to surpass diffusion models in image synthesis for the first time, although it remains limited to class-conditioned synthesis.

Another branch of models uses BERT-style masking (Chang et al., 2022; Ding et al., 2022; Chang et al., 2023; Wang et al., 2024), where random masked tokens are predicted based on token prediction. Works in this area include MagViT (Yu et al., 2023a), MaskGIT (Chang et al., 2022), MUSE (Chang et al., 2023), MagViT-2 (Yu et al., 2023b), *etc.*

### 3 METHOD

#### 3.1 PRELIMINARY: FROM “NEXT-TOKEN PREDICTION” TO “NEXT-SCALE PREDICTION”

**Next-token prediction** forms the core of traditional auto-regressive T2I models. Typically, images are tokenized by discrete tokenizers, *e.g.*, VQVAE and flattened into a series of token maps  $(x_1, x_2, \dots, x_T)$ . Prediction of each token  $x_t$  is based on the sequence of preceding tokens  $(x_1, x_2, \dots, x_{t-1})$ . The complete token map is then converted by quantizer and decoder to transform the discrete tokens into generated images.

**Next-scale prediction.** Tian et al. (2024) point out that conventional “next token prediction” task is inadequate for highly-structured, non-linguistic modalities like image, which inherently require bi-directional and 2D structural dependence. Instead, they reformulate the auto-regressive approach from token-wise to scale-wise generation. VAR begins with initial  $1 \times 1$  token map  $r_1$ , and auto-regressively predicts  $(r_1, r_2, \dots, r_K)$  with higher resolution sequentially. The sequence generation process can be formulated as multiplication of  $K$  conditional probabilities:

$$p(r_1, r_2, \dots, r_K) = \prod_{k=1}^K p(r_k | r_1, r_2, \dots, r_{k-1}) \quad (1)$$

where token map at each scale  $r_k \in [V]^{h_k \times w_k}$  is generated based on previous token maps  $(r_1, r_2, \dots, r_{k-1})$  at  $k-1$  scales. Here,  $V$  represents the VQVAE codebook, while  $h_k$  and  $w_k$  denote the height and width of token map at scale  $k$ , respectively. To construct multi-scale latent token maps for supervision, vanilla VQVAE with modified multi-scale quantization layers is constructed, and codebook  $V$  is shared across all scales.

With the alignment of scale-wise prediction scheme with the intrinsic properties of visual data, VAR significant advances previous auto-regressive works. It offers better scalability with reaching the lower bound of FID, along with increased efficiency. This breakthrough underscores the potential of auto-regressive models to produce high-quality images.

**Limitations.** Although VAR has achieved efficient conditioned generation with categories, it encounters certain limitations that hinder broader application:

- 1) *Restricted conditions.* VAR only considers generation under limited categories, posing restricted diversity in conditions and inhibits the model’s ability to generalize to new objects or concepts.
- 2) *Generating token maps across different scales.* VAR incorporates learnable absolute positional encodings (APEs) for tokens at each scale, which increases the learnable parameter and complicates optimization process, consequently limiting its capabilities under high-resolution synthesis.

### 3.2 EFFICIENT TEXTUAL GUIDANCE

In VAR, class condition serves as start token [s] at the initial scale, while a transformer with class-conditioned Adaptive Layer Normalization (AdaLN) layers is utilized to predict subsequent scales. For text-guided generation, which is an open set problem that necessitates generalization to new scenarios. Rather than jointly encoding text and images, we leverage pre-trained text encoders to acquire generalized representations. Specifically, to ensure detailed guidance for text-prompt generation while preserving diversity, we make two principal designs:

**Start tokens.** Originally, VAR relies on class embeddings tied to a predefined set of categories, thereby limiting the diversity of generated images since the start token predominantly determines the global content of output. To enhance versatility and ensure better alignment between text and images, we employ pooled text features as the start token. This change provides generalizable features, facilitating adaptation to new textual scenarios. Furthermore, it ensures consistency between textual descriptions and visual outputs.

**Fine-grained guidance at each scale.** Textual information, with its inherent complexity, presents a greater challenge compared to class conditioning, which is often limited to merely 1,000 ImageNet (Deng et al., 2009) categories. While AdaLN is adept at managing simple conditional information, e.g., timesteps in diffusion models, styles, etc.. Similarly, the start  $1 \times 1$  token also lacks the capacity to convey sufficient textual detail, and risks of being obscured in the subsequent scales.

Therefore, a new mechanism for implementing text understanding in each scale is necessary. Inspired by the success of cross-attention mechanism in diffusion models, we inject feature extracted from pre-trained text encoder with cross-attention mechanism to provide detailed textual guidance for token maps at each scale. Specifically, we insert additional cross-attention layers between self-attention and feed-forward within each transformer layer.

Through efficient pooled embedding and cross-attention mechanisms, we achieve robust consistency between images and text. For a concise overview of network structure, refer to Fig. 3.

### 3.3 NORMALIZED ROTARY POSITIONAL ENCODING

In the next-scale prediction scheme, tokens from the same scale are generated at once. Encoding the position of each token inside current scale is crucial. Existing transformers, typically utilize learnable absolute positional encoding (APEs) (Vaswani et al., 2017) or 2D sinusoidal positional encoding (Chen et al., 2023a), to mark tokens’ absolute positions in images.

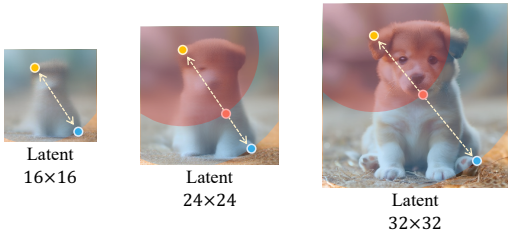


Figure 4: Illustration of confusions caused by positional encodings across scales. In different scale token maps, two points’ relative positions are different across scales, causing confusion with 2D RoPE (e.g., mistaking red points for the dog’s paw in new scales). Normalizing RoPE with each scale’s token map size ensures correct positioning (blue point for dog’s paw in every scale).

Table 1: Performance comparison under MJHQ-30K shows that our method achieves the best FID (“4.73”) and CLIP-Score (“0.291”) for 512×512 generation, with merely 2.95s per image<sup>1</sup>.

Methods	Type	FID↓		CLIP-Score↑		Infer. Time [s]
		Rank	Score	Rank	Score	
Stable Diffusion v2.1	Diff.	5	26.96	5	0.259	8.61
SDXL	Diff.	4	11.42	1	0.291	10.18
Playground v2.5	Diff.	2	6.57	4	0.283	8.96
PixArt-α	Diff.	3	6.64	3	0.284	6.48
Ours	AR	1	4.73	1	0.291	2.95

For sizes of token map at each scale varies, the existing position encodings exhibit following limitations: Firstly, flattened absolute positional encodings (APEs) fail to account for the intrinsic 2D structure of images, leading to unnecessary increases in model parameters. This issue becomes more pronounced when generating images at larger scales. Moreover, sinusoidal encodings struggle to adapt when dealing with sequences of different lengths, which is sub-optimal for modeling varying token maps across scales. A slight change of size in token map renders a significant distortion, and forcibly learning with inconsistent positional embeddings for different scales can lead to potential confusion. For instance, two points that are equidistant in token maps with different scales, yet may cause confusion due to their differing interpretations caused by the varying shapes of scales, See Fig. 4 for example.

To address this inconsistency and more effectively encode 2D information, we propose *normalized 2D Axial Rotary Position Encoding (RoPE)* to better model image features based on the relative positions of tokens with consistent representations across different scales. For a given scale  $k$ , a 2D grid with size  $h_k \times w_k$  is constructed, for position  $(i, j), i \in \{1, 2, \dots, h_k\}, j \in \{1, 2, \dots, w_k\}$ , the normalized 2D rotary positional encoding  $PE(i, j)$  is calculated based on normalized grid with token map size of the current scale  $h_k \times w_k$ :

$$PE(i, j) = \text{RoPE}_x\left(\frac{i}{h_k} \cdot H\right) \oplus \text{RoPE}_y\left(\frac{j}{w_k} \cdot W\right) \tag{2}$$

Here  $H$  and  $W$  are multiplied on normalized grid to produce more distinguishable distances, usually satisfy  $H > h_K$  and  $W > w_K$ . The  $\oplus$  denotes concatenation in channel dimension, and  $\text{RoPE}_x(\cdot)$  and  $\text{RoPE}_y(\cdot)$  represent the rotary embeddings for  $x$  and  $y$  dimensions, respectively.

With this normalized relative positional encoding to model the spatial relationships of tokens, all scale token maps are recognized as latents of the same normalized size, *i.e.*,  $(H \times W)$ , with relative positions. This approach ensures consistency across positions at different scales, which allows the model to utilize encoded positional information to better predict the token maps at new scales.

## 4 EXPERIMENT

### 4.1 IMPLEMENTATION DETAILS

**Model parameters.** Follow Tian et al. (2024), we adopt a standard decoder-only transformer architecture similar to Radford et al. (2019), and adhere to the model shape hyper-parameter rules outlined in Kaplan et al. (2020). Specifically, the main parameter count  $N$  of the transformer scales as  $O(d^3)$  with depth  $d$ . Our implementation is based on the VAR configuration with  $d = 30$ , resulting in approximately 1.7 billion parameters, leveraging scalability to enhance text-to-image generation capabilities. Additionally, we utilize the same CLIP text encoder as Stable Diffusion v2.1, which features a ViT-L/14 backbone, supporting up to 77 tokens and a latent channel width of 1024. More powerful language models, such as T5, can bring further performance gains.

**Datasets.** The training datasets are sourced from JourneyDB, LAION-HD, and LAION-Art. Since the captions provided by LAION-HD and LAION-Art do not adequately describe the image content,

<sup>1</sup>For official models of SDXL and Playground v2.5 are trained on 1024×1024 images, we utilize a fine-tuned version of SDXL: <https://huggingface.co/hotshotco/SDXL-512>, and their 1024 results are provided for reference (“9.55” for SDXL and “4.48” for Playground v2.5)

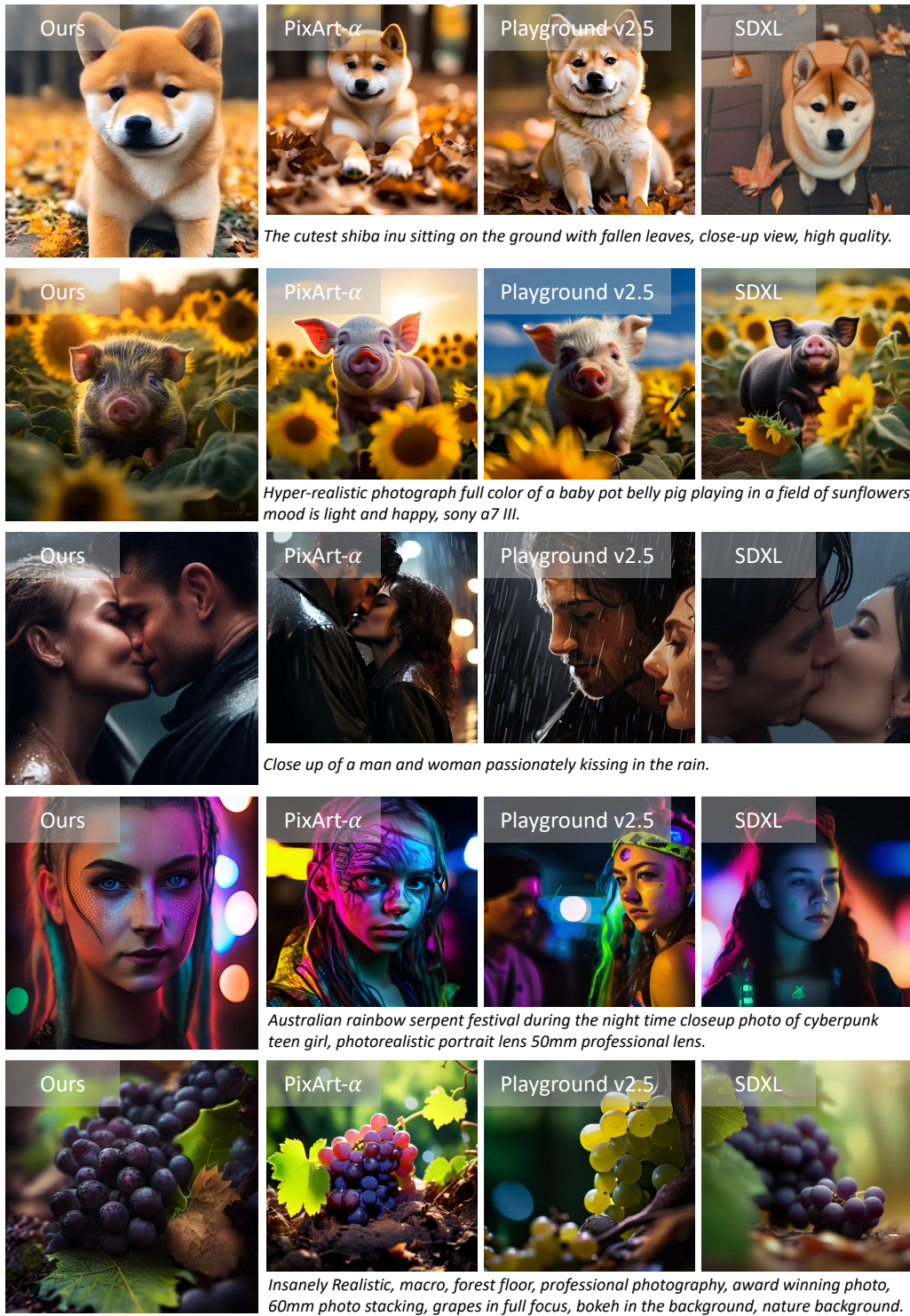


Figure 5: Qualitative comparison between STAR and other SOTA models.

we use ShareGPT4v (Chen et al., 2023b) to recaption them. The images are center-cropped and proportionally resized to fit the training dimensions.

**Training Details.** During training, the transformer predicts concatenated token maps for all scales along the length dimension, resulting in an attention map of size  $(\sum_{k=1}^K h_k \times w_k) \times (\sum_{k=1}^K h_k \times w_k)$ .

This approach significantly increases computation costs, especially for larger images. To manage this, we first train on  $256 \times 256$  images with larger batch size, then fine-tune on  $512 \times 512$  images with smaller batch size for 512 resolution. With normalized RoPE providing consistency across different scales, the network adapts quickly to new dimensions during training, leading to rapid convergence.

4.2 PERFORMANCE COMPARISONS AND ANALYSIS

**Models.** We thoroughly compare STAR with existing leading methods, including Stable Diffusion v2.1 (Rombach et al., 2022) (“SD v2.1”), SDXL (Podell et al., 2023), Playground v2.5 (Li et al., 2024) and PixArt- $\alpha$  (Chen et al., 2023a). All models are systematically evaluated in terms of fidelity (“FID”), image-text consistency (“CLIP-Score”) and human preferences (“ImageReward”).

**Fidelity.** FID Measure the discrepancy between the distributions of generated images and real images. Noting the discrepancy between COCO validation set styles and practical preferences, we use the MJHQ-30k benchmark proposed by Playground (Li et al., 2024) for evaluation. Additionally, we use ImageReward (Xu et al., 2024) to assess human preference for the generated images. As shown in Table 1, STAR achieves the best FID of 4.73 with significantly reduced inference time of <3 seconds, compared to those who requires around 10 second. Notably, STAR can produce incredible details, as shown in Fig. 5, especially in fur, hair, facial features, and plant leaves.

**Text Image Alignment.** Beyond the above evaluation, we also report CLIP-Score (See Table 1, 2), which indicates the correlation between textual prompts and generated images. STAR achieves the best alignment performance, benefiting from the efficient collaboration of cross-attention and start tokens.

**Human Preferences.** Additionally, we use ImageReward (Xu et al., 2024) to assess human preference for generated images. This comprehensive criterion measures human aesthetic preferences, body proportions, and other factors based on pre-trained BLIP model. Results are listed in Table 2.

Table 2: Performance on ImageReward benchmark. Our model is comparable with the best.

Methods	ImageReward $\uparrow$		CLIP-Score $\uparrow$	
	Rank	Score	Rank	Score
SD v2.1	5	0.2457	5	0.2683
SDXL	4	0.4155	2	0.2822
Playground v2.5	3	0.6925	4	0.2767
PixArt- $\alpha$	1	0.9037	3	0.2780
Ours	2	0.8660	1	0.2865

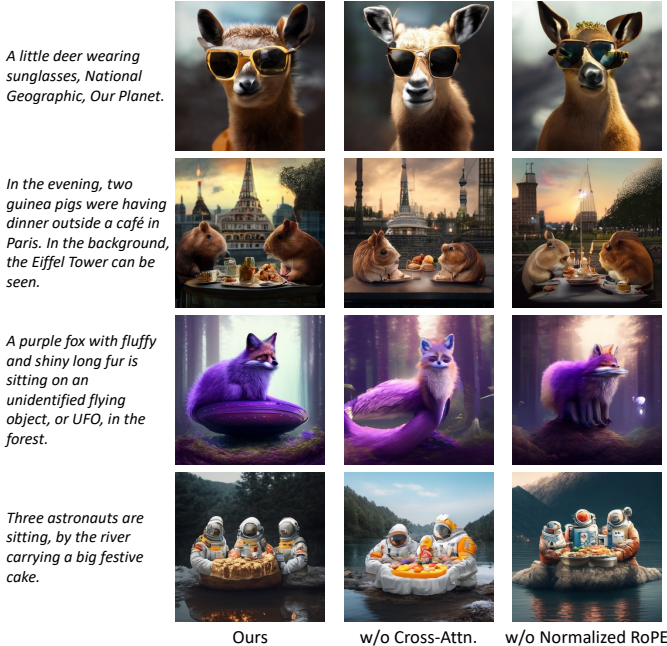


Figure 6: Illustration of ablations. No cross attention makes understanding complex scenes difficult (e.g., counting, object relationships). Replacing normalized RoPE with learnable APE hinders position learning, causing shape distortions.



### 4.3 ABLATION STUDY

**Normalized RoPE.** To illustrate the effectiveness of the proposed normalized RoPE, we replace it with learnable absolute positional encodings in the  $depth=16$  model. As shown in “w/o Normalized RoPE” of Fig. 6, the model will be difficult to train and is prone to deformation.

**Cross-Attention.** We provide text guidance through pooled features and cross-attention. Using only pooled features as start tokens is insufficient, as it fails to adequately express complex textual information, impacting the generation across all scales. The results of removing cross-attention, shown in “w/o Cross-Attn.” in Fig. 6, demonstrate confusion in understanding complex scenes involving counting, spatial relations, and multiple objects.

**Scaling-up parameters.** Auto-regressive transformers exhibit superior scalability, allowing for performance enhancements through increased model parameters. By scaling up model from  $depth=16$  (“d16”) to  $depth=30$  (“d30”), a marked improvement in performance metrics is observed, as illustrated in Table 3. This scaling behavior highlights the inherent advantage of auto-regressive transformers in benefiting from additional parameters.

Table 3: Results under different sizes ( $256 \times 256$  and  $512 \times 512$  and different model scales (depth-16 and depth-30).

Depth	#Reso	#Param	CLIP-score $\uparrow$	FID $\downarrow$
16	256	274M	0.272	6.88
30	256	1.68B	0.286	5.19
30	512	1.68B	0.291	4.73

## 5 FUTURE WORKS

In this work, we focus on new auto-regressive generative paradigm, *i.e.*, “next-scale prediction”, for efficient high-quality text-to-image generation. However, there are still some areas for improvement:

**Higher resolutions.** Due to the limitations of the current training method, generating larger scale images requires significantly more computational resources. Currently, we can generate images at resolutions of  $256 \times 256$  and  $512 \times 512$ . We are developing more efficient training strategies to enable larger scale generation, such as  $1024 \times 1024$ . Additionally, the inherent limitations of multi-scale VQVAE and the single-scale training strategy restrict our current model to generating images at a single resolution, resulting in limited usability. We will explore a mixed-resolution training strategy to allow the model to adapt to a wider range of resolutions.

**More efficient sampling strategy.** In our current generation pipeline, the process involves starting from a specific semantic start token and gradually generating higher resolution tokens guided by the text. The randomness in generation comes from top-k sampling of predicted token indexes. We believe there is room for improvement to generate more diverse and detail-rich images.

**Downstream tasks.** Unlike diffusion models, our approach uses auto-regressive generation. Whether it can support a wide range of downstream tasks, such as controllable generation and image editing, similar to diffusion models, remains an open question for future exploration.

## 6 CONCLUSION

In this work, we explore a new auto-regressive paradigm, namely “next-scale prediction,” for efficient text-to-image (T2I) synthesis. Our approach, STAR, predicts discrete latent space feature maps in a scale-wise manner, using pooling features and cross-attention for text guidance. Additionally, it employs normalized RoPE to avoid positional confusion across different scales and efficiently encodes token positions, enabling higher resolution generation.

STAR achieves superior performance in terms of fidelity, text-image alignment, and human preference. Remarkably, it generates a high-quality  $512 \times 512$  image with stunning details in approximately 2.9 seconds. Compared to the leading diffusion models in the T2I domain, STAR offers significant time advantages and produces images with greater detail, presenting a promising new direction in the currently diffusion-dominated field of text-to-image generation.

## REFERENCES

- Tim Brooks, Bill Peebles, Connor Holmes, Will DePue, Yufei Guo, Li Jing, David Schnurr, Joe Taylor, Troy Luhman, Eric Luhman, Clarence Ng, Ricky Wang, and Aditya Ramesh. Video generation models as world simulators. 2024. URL <https://openai.com/research/video-generation-models-as-world-simulators>.
- Tom Brown, Benjamin Mann, Nick Ryder, Melanie Subbiah, Jared D Kaplan, Prafulla Dhariwal, Arvind Neelakantan, Pranav Shyam, Girish Sastry, Amanda Askell, et al. Language models are few-shot learners. *Advances in neural information processing systems*, 33:1877–1901, 2020.
- Huiwen Chang, Han Zhang, Lu Jiang, Ce Liu, and William T Freeman. Maskgit: Masked generative image transformer. In *Proceedings of the IEEE/CVF Conference on Computer Vision and Pattern Recognition*, pp. 11315–11325, 2022.
- Huiwen Chang, Han Zhang, Jarred Barber, AJ Maschinot, Jose Lezama, Lu Jiang, Ming-Hsuan Yang, Kevin Murphy, William T Freeman, Michael Rubinstein, et al. Muse: Text-to-image generation via masked generative transformers. *arXiv preprint arXiv:2301.00704*, 2023.
- Junsong Chen, Jincheng Yu, Chongjian Ge, Lewei Yao, Enze Xie, Yue Wu, Zhongdao Wang, James Kwok, Ping Luo, Huchuan Lu, et al. Pixart- $\alpha$ : Fast training of diffusion transformer for photorealistic text-to-image synthesis. *arXiv preprint arXiv:2310.00426*, 2023a.
- Junsong Chen, Chongjian Ge, Enze Xie, Yue Wu, Lewei Yao, Xiaoze Ren, Zhongdao Wang, Ping Luo, Huchuan Lu, and Zhenguo Li. Pixart- $\Sigma$ : Weak-to-strong training of diffusion transformer for 4k text-to-image generation. *arXiv preprint arXiv:2403.04692*, 2024.
- Lin Chen, Jisong Li, Xiaoyi Dong, Pan Zhang, Conghui He, Jiaqi Wang, Feng Zhao, and Dahua Lin. Sharegpt4v: Improving large multi-modal models with better captions. *arXiv preprint arXiv:2311.12793*, 2023b.
- Jia Deng, Wei Dong, Richard Socher, Li-Jia Li, Kai Li, and Li Fei-Fei. Imagenet: A large-scale hierarchical image database. In *2009 IEEE conference on computer vision and pattern recognition*, pp. 248–255. Ieee, 2009.
- Prafulla Dhariwal and Alexander Nichol. Diffusion models beat gans on image synthesis. *Advances in neural information processing systems*, 34:8780–8794, 2021.
- Ming Ding, Wendi Zheng, Wenyi Hong, and Jie Tang. Cogview2: Faster and better text-to-image generation via hierarchical transformers. *Advances in Neural Information Processing Systems*, 35:16890–16902, 2022.
- Patrick Esser, Robin Rombach, and Bjorn Ommer. Taming transformers for high-resolution image synthesis. In *Proceedings of the IEEE/CVF conference on computer vision and pattern recognition*, pp. 12873–12883, 2021.
- Patrick Esser, Sumith Kulal, Andreas Blattmann, Rahim Entezari, Jonas Müller, Harry Saini, Yam Levi, Dominik Lorenz, Axel Sauer, Frederic Boesel, et al. Scaling rectified flow transformers for high-resolution image synthesis. *arXiv preprint arXiv:2403.03206*, 2024.
- Oran Gafni, Adam Polyak, Oron Ashual, Shelly Sheynin, Devi Parikh, and Yaniv Taigman. Make-a-scene: Scene-based text-to-image generation with human priors. In *European Conference on Computer Vision*, pp. 89–106. Springer, 2022.
- Jonathan Ho and Tim Salimans. Classifier-free diffusion guidance. *arXiv preprint arXiv:2207.12598*, 2022.
- Minguk Kang, Jun-Yan Zhu, Richard Zhang, Jaesik Park, Eli Shechtman, Sylvain Paris, and Taesung Park. Scaling up gans for text-to-image synthesis. In *Proceedings of the IEEE/CVF Conference on Computer Vision and Pattern Recognition*, pp. 10124–10134, 2023.
- Jared Kaplan, Sam McCandlish, Tom Henighan, Tom B Brown, Benjamin Chess, Rewon Child, Scott Gray, Alec Radford, Jeffrey Wu, and Dario Amodei. Scaling laws for neural language models. *arXiv preprint arXiv:2001.08361*, 2020.

- Tero Karras, Samuli Laine, and Timo Aila. A style-based generator architecture for generative adversarial networks. In *Proceedings of the IEEE/CVF conference on computer vision and pattern recognition*, pp. 4401–4410, 2019.
- Tero Karras, Samuli Laine, Miika Aittala, Janne Hellsten, Jaakko Lehtinen, and Timo Aila. Analyzing and improving the image quality of stylegan. In *Proceedings of the IEEE/CVF conference on computer vision and pattern recognition*, pp. 8110–8119, 2020.
- JDMCK Lee and K Toutanova. Pre-training of deep bidirectional transformers for language understanding. *arXiv preprint arXiv:1810.04805*, 3:8, 2018.
- Daiqing Li, Aleks Kamko, Ehsan Akhgari, Ali Sabet, Linmiao Xu, and Suhail Doshi. Playground v2. 5: Three insights towards enhancing aesthetic quality in text-to-image generation. *arXiv preprint arXiv:2402.17245*, 2024.
- Simian Luo, Yiqin Tan, Longbo Huang, Jian Li, and Hang Zhao. Latent consistency models: Synthesizing high-resolution images with few-step inference. *arXiv preprint arXiv:2310.04378*, 2023.
- OpenAI. Dalle-2, 2023. URL <https://openai.com/dall-e-2>.
- William Peebles and Saining Xie. Scalable diffusion models with transformers. In *Proceedings of the IEEE/CVF International Conference on Computer Vision*, pp. 4195–4205, 2023.
- Dustin Podell, Zion English, Kyle Lacey, Andreas Blattmann, Tim Dockhorn, Jonas Müller, Joe Penna, and Robin Rombach. Sdxl: Improving latent diffusion models for high-resolution image synthesis. In *The Twelfth International Conference on Learning Representations*, 2023.
- Alec Radford, Jeffrey Wu, Rewon Child, David Luan, Dario Amodei, Ilya Sutskever, et al. Language models are unsupervised multitask learners. *OpenAI blog*, 1(8):9, 2019.
- Aditya Ramesh, Mikhail Pavlov, Gabriel Goh, Scott Gray, Chelsea Voss, Alec Radford, Mark Chen, and Ilya Sutskever. Zero-shot text-to-image generation. In *International conference on machine learning*, pp. 8821–8831. Pmlr, 2021.
- Robin Rombach, Andreas Blattmann, Dominik Lorenz, Patrick Esser, and Björn Ommer. High-resolution image synthesis with latent diffusion models. In *Proceedings of the IEEE/CVF conference on computer vision and pattern recognition*, pp. 10684–10695, 2022.
- Chitwan Saharia, William Chan, Saurabh Saxena, Lala Li, Jay Whang, Emily L Denton, Kamyar Ghasemipour, Raphael Gontijo Lopes, Burcu Karagol Ayan, Tim Salimans, et al. Photorealistic text-to-image diffusion models with deep language understanding. *Advances in neural information processing systems*, 35:36479–36494, 2022.
- Victor Sanh, Albert Webson, Colin Raffel, Stephen H Bach, Lintang Sutawika, Zaid Alyafeai, Antoine Chaffin, Arnaud Stiegler, Teven Le Scao, Arun Raja, et al. Multitask prompted training enables zero-shot task generalization. *arXiv preprint arXiv:2110.08207*, 2021.
- Jiaming Song, Chenlin Meng, and Stefano Ermon. Denoising diffusion implicit models. *arXiv preprint arXiv:2010.02502*, 2020.
- Jianlin Su, Murtadha Ahmed, Yu Lu, Shengfeng Pan, Wen Bo, and Yunfeng Liu. Roformer: Enhanced transformer with rotary position embedding. *Neurocomputing*, 568:127063, 2024.
- Ming Tao, Hao Tang, Songsong Wu, Nicu Sebe, Xiao-Yuan Jing, Fei Wu, and Bingkun Bao. Df-gan: Deep fusion generative adversarial networks for text-to-image synthesis. *arXiv preprint arXiv:2008.05865*, 2(6), 2020.
- Keyu Tian, Yi Jiang, Zehuan Yuan, Bingyue Peng, and Liwei Wang. Visual autoregressive modeling: Scalable image generation via next-scale prediction. *arXiv preprint arXiv:2404.02905*, 2024.
- Hugo Touvron, Thibaut Lavril, Gautier Izacard, Xavier Martinet, Marie-Anne Lachaux, Timothée Lacroix, Baptiste Rozière, Naman Goyal, Eric Hambro, Faisal Azhar, et al. Llama: Open and efficient foundation language models. *arXiv preprint arXiv:2302.13971*, 2023a.

- Hugo Touvron, Louis Martin, Kevin Stone, Peter Albert, Amjad Almahairi, Yasmine Babaei, Nikolay Bashlykov, Soumya Batra, Prajjwal Bhargava, Shruti Bhosale, et al. Llama 2: Open foundation and fine-tuned chat models. *arXiv preprint arXiv:2307.09288*, 2023b.
- Aaron Van Den Oord, Oriol Vinyals, et al. Neural discrete representation learning. *Advances in neural information processing systems*, 30, 2017.
- Ashish Vaswani, Noam Shazeer, Niki Parmar, Jakob Uszkoreit, Llion Jones, Aidan N Gomez, Łukasz Kaiser, and Illia Polosukhin. Attention is all you need. *Advances in neural information processing systems*, 30, 2017.
- Xiaofeng Wang, Zheng Zhu, Guan Huang, Boyuan Wang, Xinze Chen, and Jiwen Lu. World-dreamer: Towards general world models for video generation via predicting masked tokens. *arXiv preprint arXiv:2401.09985*, 2024.
- Jiazheng Xu, Xiao Liu, Yuchen Wu, Yuxuan Tong, Qinkai Li, Ming Ding, Jie Tang, and Yuxiao Dong. Imagereward: Learning and evaluating human preferences for text-to-image generation. *Advances in Neural Information Processing Systems*, 36, 2024.
- Tao Xu, Pengchuan Zhang, Qiuyuan Huang, Han Zhang, Zhe Gan, Xiaolei Huang, and Xiaodong He. Attngan: Fine-grained text to image generation with attentional generative adversarial networks. In *Proceedings of the IEEE conference on computer vision and pattern recognition*, pp. 1316–1324, 2018.
- Jiahui Yu, Xin Li, Jing Yu Koh, Han Zhang, Ruoming Pang, James Qin, Alexander Ku, Yuanzhong Xu, Jason Baldridge, and Yonghui Wu. Vector-quantized image modeling with improved vqgan. *arXiv preprint arXiv:2110.04627*, 2021.
- Jiahui Yu, Yuanzhong Xu, Jing Yu Koh, Thang Luong, Gunjan Baid, Zirui Wang, Vijay Vasudevan, Alexander Ku, Yinfei Yang, Burcu Karagol Ayan, et al. Scaling autoregressive models for content-rich text-to-image generation. *arXiv preprint arXiv:2206.10789*, 2(3):5, 2022a.
- Jiahui Yu, Yuanzhong Xu, Jing Yu Koh, Thang Luong, Gunjan Baid, Zirui Wang, Vijay Vasudevan, Alexander Ku, Yinfei Yang, Burcu Karagol Ayan, et al. Scaling autoregressive models for content-rich text-to-image generation. *arXiv preprint arXiv:2206.10789*, 2(3):5, 2022b.
- Lijun Yu, Yong Cheng, Kihyuk Sohn, José Lezama, Han Zhang, Huiwen Chang, Alexander G Hauptmann, Ming-Hsuan Yang, Yuan Hao, Irfan Essa, et al. Magvit: Masked generative video transformer. In *Proceedings of the IEEE/CVF Conference on Computer Vision and Pattern Recognition*, pp. 10459–10469, 2023a.
- Lijun Yu, José Lezama, Nitesh B Gundavarapu, Luca Versari, Kihyuk Sohn, David Minnen, Yong Cheng, Agrim Gupta, Xiuye Gu, Alexander G Hauptmann, et al. Language model beats diffusion-tokenizer is key to visual generation. *arXiv preprint arXiv:2310.05737*, 2023b.
- Lvmin Zhang, Anyi Rao, and Maneesh Agrawala. Adding conditional control to text-to-image diffusion models. In *Proceedings of the IEEE/CVF International Conference on Computer Vision*, pp. 3836–3847, 2023.
- Susan Zhang, Stephen Roller, Naman Goyal, Mikel Artetxe, Moya Chen, Shuohui Chen, Christopher Dewan, Mona Diab, Xian Li, Xi Victoria Lin, et al. Opt: Open pre-trained transformer language models. *arXiv preprint arXiv:2205.01068*, 2022.